Journal of Medicinal Chemistry

Article

pubs.acs.org/jmc

Acyclic Cucurbit[*n*]uril-type Molecular Containers: Influence of Aromatic Walls on their Function as Solubilizing Excipients for Insoluble Drugs

Ben Zhang and Lyle Isaacs*

Department of Chemistry and Biochemistry, University of Maryland, College Park, Maryland 20742, United States

Supporting Information

ABSTRACT: We studied the influence of the aromatic sidewalls on the ability of acyclic CB[*n*]-type molecular containers (**1a**−**1e**) to act as solubilizing agents for 19 insoluble drugs including the developmental anticancer agent PBS-1086. All five containers exhibit good water solubility and weak self-association ($K_s \leq 624\ M^{-1}$). We constructed phase solubility diagrams to extract K_{rel} and K_a values for the container·drug complexes. The acyclic CB[*n*]-type containers generally display significantly higher K_a values than HP-*β*-CD toward drugs. Containers **1a**−**1e** bind the steroidal ring system and aromatic moieties of insoluble drugs. Compound **1b** displays highest affinity toward most of the drugs studied. Containers **1a** and **1b** are broadly applicable and can be used to formulate a wider variety of insoluble drugs than was previously possible with cyclodextrin technology. For drugs that are solubilized by both HP-*β*-CD and **1a**−**1e**, lower concentrations of **1a**−**1e** are required to achieve identical [drug].

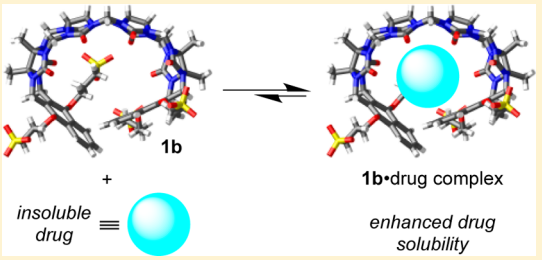

INTRODUCTION

Molecular container compounds have been extensively studied over the years by synthetic, supramolecular, materials, and medicinal chemists by virtue of their ability to alter the properties of compounds bound within their interior. Some of the best-investigated classes of molecular container compounds include crown ethers, cryptands, carcerands, calixarenes, cyclophanes, cyclodextrins, and complexes self-assembled by metal·ligand and H-bonding interactions as well as reversible covalent bonds.[1] For example, encapsulation inside molecular containers can reduce the reactivity of highly reactive species like P_4, reduce the odor of malodorous compounds, promote the reactions of included substrates, provide the basis of stimuli responsive molecular machines, enhance the photophysical properties of encapsulated dyes, and even reverse the toxic effects of certain compounds.[1f,2] We, and others, have been studying an alternative class of molecular containers known as cucurbit[*n*]urils (CB[*n*], *n* = 5, 6, 7, 8, 10, Figure 1).[3] CB[*n*] compounds are particularly attractive because of the remarkably high affinity, selectivity, and stimuli responsiveness that they display toward their guests in aqueous solution.[4] For these reasons, CB[*n*] compounds have been used as key components in the construction of functional supramolecular systems including affinity separation phases, supramolecular velcro, surface enhanced Raman scattering sensing, and for biomembrane assays.[5]

An urgent problem facing the pharmaceutical industry is that a high percentage of new chemical entities with documented target affinity are so poorly soluble that formulation is challenging.[6] A number of techniques and tools have been developed to address the drug solubility issue including the generation of nanocrystalline solid forms of the drug, salt formation, solid dispersions, and higher solubility prodrugs.[7] Of highest relevance to supramolecular chemists, however, is the

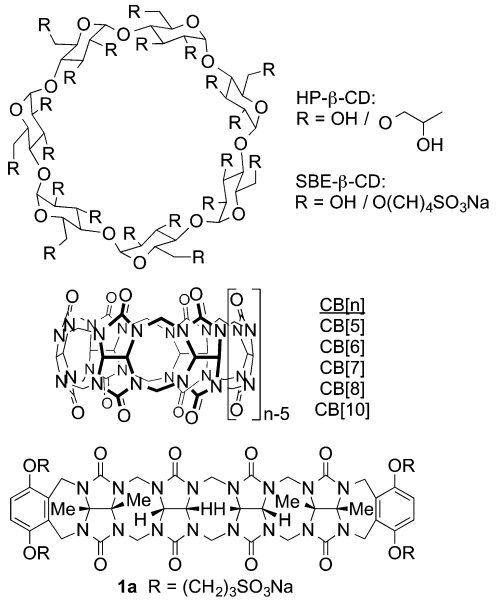

Figure 1. Structures of molecular containers used previously as solubilizing agents for insoluble drugs: HP-*β*-CD, SBE-*β*-CD, CB[*n*], and acyclic CB[*n*]-type container **1a**.

Received: August 20, 2014
Published: November 4, 2014

Scheme 1. Structures of Known Acyclic CB[*n*] Solubilizing Excipients 1b and 1c and Synthesis of 1d and 1e

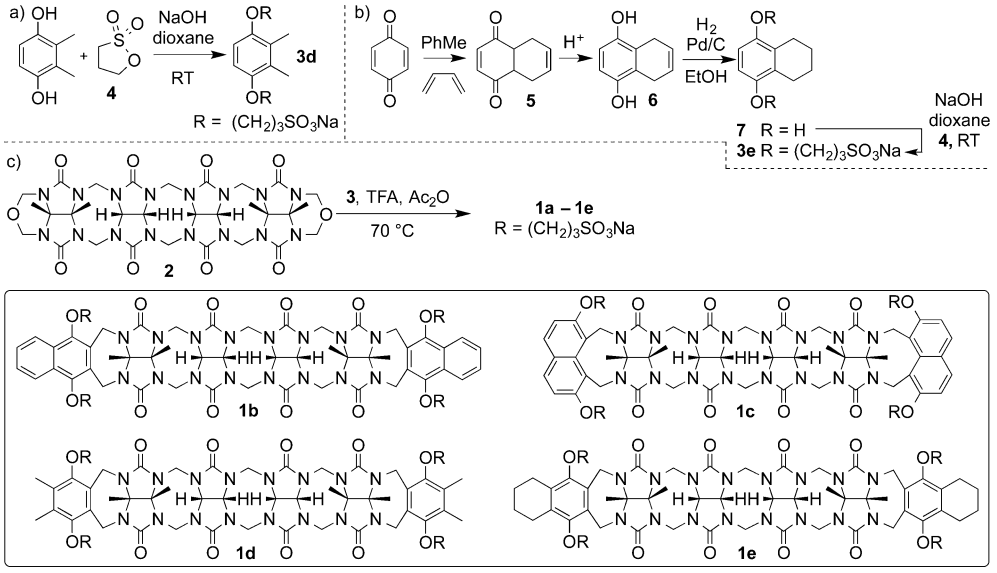

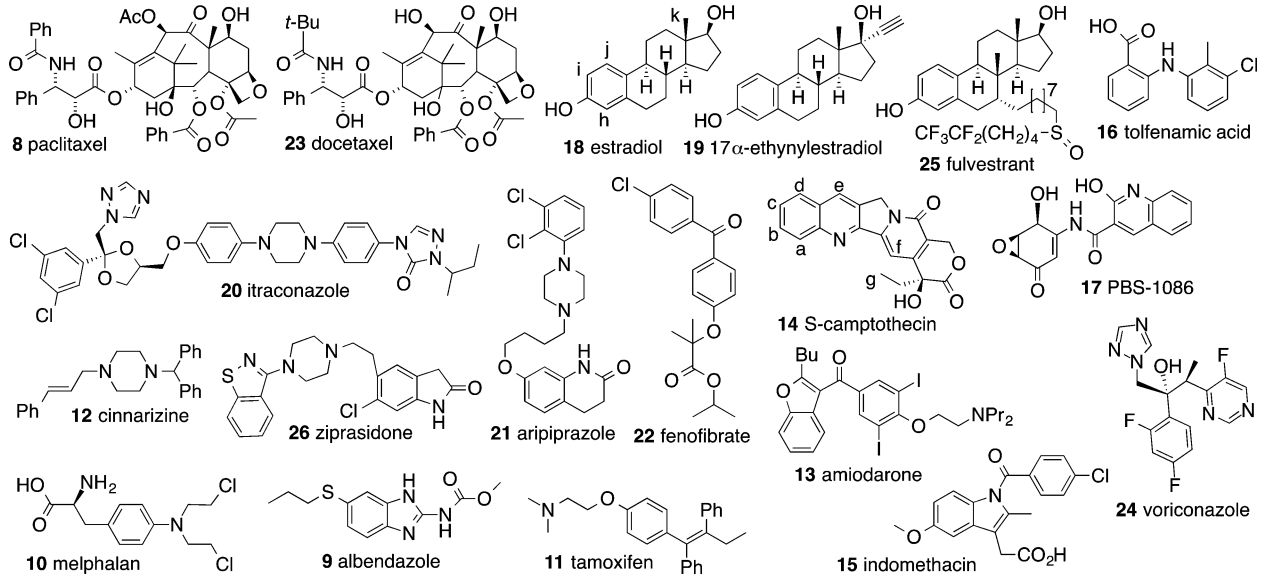

Figure 2. Chemical structures of drugs used in this study.

use of the cyclodextrin derivatives hydroxypropyl-*β*-cyclodextrin (HP-*β*-CD) and sulfobutyl ether-*β*-cyclodextrin (SBE-*β*-CD, Figure 1) to improve the solubility of insoluble drugs by encapsulation inside the molecular containers.[8] A number of drugs are formulated for administration to humans by encapsulation inside HP-*β*-CD and SBE-*β*-CD. Accordingly, researchers in the CB[*n*] area are exploring their use in this class of applications. For example, CB[*n*] have been used to increase the solubility of a number of insoluble drugs (e.g., albendazole, chlorambucil, camptothecin), to retard degradation reactions, and for targeted drug delivery.[9]

The Isaacs group has been interested in understanding the mechanism of CB[*n*] formation and using that information to prepare CB[*n*]-type receptors with new structural features and recognition properties.[10] In 2012, we reported the synthesis of acyclic CB[*n*]-type receptor **1a** and its use as a solubilizing excipient for insoluble drugs. Compound **1a** and relatives have three main structural features: (1) a central glycoluril oligomer to impart curvature and the ability to bind to hydrophobic and cationic species, (2) terminal aromatic walls to promote $\pi-\pi$ interactions between container and insoluble drug, and (3) solubilizing sulfonate arms that result in high solubility.[11] Compound **1a** is not toxic in *in vitro* and *in vivo* assays, and paclitaxel (**8**) formulated as **1a**·paclitaxel maintains its ability to efficiently kill HeLa cells.[11c] We also showed that acyclic CB[*n*]-type container **1b** and relatives are capable of *in vivo* reversal (in rats) of the biological effects of rocuronium which is a neuromuscular blocking agent commonly used by anesthesiologists during surgery.[11d] Previously, we studied the influence of the nature of the solubilizing groups (e.g., SO_3^- vs OH vs NH_3^+) on the ability of acyclic CB[*n*] type containers to act as solubilizing agents for insoluble drugs and found that sulfonate groups are particularly well-suited for this application because they impart high solubility in water and do not promote self-folding and complexation (e.g., as NH_3^+ does).[12] In this Article we explore the influence of the nature of the aromatic sidewalls on the ability of the acyclic CB[*n*]-type

dx.doi.org/10.1021/jm501276u | J. Med. Chem. 2014, 57, 9554−9563

containers (**1a**−**1e**, Scheme 1) to act as solubilizing agents for insoluble drugs.

RESULTS AND DISCUSSION

This Results and Discussion section is organized as follows. First, we describe the synthesis and solubility of two new acyclic CB[*n*]-type receptors **1d** and **1e**. Next, we investigate the self-association properties of **1a**−**1e**. Subsequently, we create phase solubility diagrams (PSDs) for **1a**−**1e** toward a range of well-known poorly soluble pharmaceutical agents (Figure 2) and analyze trends in the solubilization data.

Design and Synthesis of Acyclic CB[*n*]-type Containers 1a−1e. Previously, we reported the synthesis and application of acyclic CB[*n*] type containers **1a**−**1c** by the double electrophilic aromatic substitution reaction of glycoluril tetramer bis(cyclic ether) building block **2** with the corresponding dialkoxyaromatic sidewalls **3** in hot CF_3CO_2H.[11c,e,12] Compounds **1a**−**1e** differ in the nature of their aromatic sidewalls (e.g., benzene, naphthalene, tetrahydronaphthalene). These structural differences impact the conformation of the uncomplexed container (e.g., smaller, larger, taller cavity) and the type and balance of noncovalent interactions (e.g., $\pi-\pi$ versus dispersion interactions) that form in the container·drug complexes. For example, the X-ray crystal structures of **1a** show that the tips of the substituted benzene sidewalls are in close contact with one another.[11c] Therefore, to accommodate the longer naphthalene sidewalls of **1b**, the glycoluril tetramer backbone of **1b** flexes which results in a larger cavity that is defined in larger part by the aromatic naphthalene sidewalls.[11c] Compound **1c** is an isomer of **1b**; in this case the sidewalls are shorter and deeper by virtue of the attachment at the naphthalene 1,8 positions.[11e] To prepare new acyclic CB[*n*] type receptors **1d** and **1e** which possess alkyl substituted sidewalls we needed to prepare compounds **3d** and **3e**. Accordingly, we reacted 2,3-dimethylhydroquinone with 1,3-propane sultone (**4**) under basic conditions (NaOH) in dioxane at room temperature to give **3d** in 73% yield (Scheme 1a). Sidewall **3e** was prepared by a multistep procedure (Scheme 1b). First, we performed the Diels−Alder reaction between benzoquinone and 1,3-butadiene in toluene to give **5** in 92% yield.[13] Next, we aromatized **5** by treatment with HBr to give **6** in 82% yield.[13] Subsequently, we reduced the double bond of **6** under standard conditions to give **7** in 85% yield.[14] Finally, **7** was reacted with **4** under basic conditions to give the required aromatic wall **3e** in 60% yield. The reaction of glycoluril tetramer **2** with sidewall **3d** (4 equiv) in a 1:1 (v:v) mixture of TFA:Ac_2O at 70 °C gave acyclic CB[*n*] type container **1d** in 43% yield. Similarly, the reaction of **2** with **3e** (4 equiv) gave container **1e** in 30% yield.

Solubility Properties of the Acyclic CB[*n*]-type Containers 1a−1e. An important property of a container that is to be used as a solubilizing excipient for insoluble drugs is the inherent solubility of the container alone. Previously, we have reported the solubility of **1a** and **1b** in 20 mM sodium phosphate buffered D_2O at pD 7.4 as 105 and 14 mM, respectively. We used the methodology reported previously,[11c,12] ^{1}H NMR assay in the presence of 1,3,5-benzene tricarboxylic acid as internal standard of known concentration, to determine the inherent solubilities of **1c** (115 mM), **1d** (353 mM), and **1e** (145 mM). The high solubilities of **1a**, **1c**, **1d**, and **1e** make them particularly attractive as solubilizing excipients for insoluble drugs.

Self-Association Properties of Acyclic CB[*n*]-type Containers 1a−1e. Previously, we have investigated the self-association of **1a** and **1b** by dilution experiments monitored by ^{1}H NMR spectroscopy. We found that the observed changes in chemical shift for each container fit well to a 2-fold self-association model and extracted the corresponding self-association constants (**1a**, K_s = 47 M^{-1}; **1b**, K_s = 624 M^{-1}).[11c,15] Because **1a** and **1b** have a low propensity to self-associate, they are well-suited to act as solubilizing excipients for insoluble drugs. In a similar manner, we performed the ^{1}H NMR dilution experiment (15−0.1 mM) for **1d** and measured the corresponding value of K_s for **1d** as 130 M^{-1}. When we performed similar ^{1}H NMR dilution experiments for **1c**, we unexpectedly observed two sets of resonances that were in slow exchange on the chemical shift time scale. We measured the diffusion coefficients for these two species by diffusion ordered NMR spectroscopy (D = 2.058 and 1.751 × 10^{-10} m^2/s, Supporting Information) which allows us to conclude that the two species correspond to monomer **1c** and dimer $(\mathbf{1c})_2$. Accordingly, we integrated the resonances for the two species at several different concentrations and determined the value of K_s (372 M^{-1}) in the usual manner.[16] Finally, we performed a dilution experiment for **1e** (35−0.2 mM) and observed both broadening and changes in ^{1}H NMR chemical shifts. Unfortunately, the changes in chemical shift could not be fitted to the standard 2-fold self-association model, and we believe that **1e** undergoes more complex higher order aggregation. The generally weak self-association observed for **1a**−**1e** is advantageous toward their use as solubilizing excipients for insoluble drugs because the container is free to associate with drug without having to overcome strong self-assocation.

Theoretical Treatment of Phase Solubility Diagrams. PSDs are plots of [Drug] as a function of [Container] that are commonly used to study the ability of molecular containers to increase the solubility of insoluble drugs.[15,17] These PSDs can assume a variety of shapes, but linear PSDs (A_L-type) are most common and occur when container and guest form soluble well-defined 1:1 container·guest complexes. Such PSDs behave according to eq 1 where S_0 is the solubility of drug alone and K_a is the binding constant for the container·drug complex. The slope of an A_L-type PSD simply reflects the ratio of the increase in concentration of drug obtained relative to the concentration of container used. Container·drug systems that display larger PSD slopes (e.g., slope ≥0.5) are advantageous because larger concentrations of drug can be obtained with smaller concentrations of container. Figure 3 shows the results of two simulations that were performed on a hypothetical container·drug system that obeys eq 1 to stimulate the discussion and analysis of the experimental PSDs created for containers **1a**−**1e** and HP-β-CD with drugs **8**−**26** shown in Figure 2. Figure 3a shows the calculated PSDs for five different containers and a single drug with S_0 = 1 × 10^{-6} M which form well-defined 1:1 container·drug complexes of high solubility. The different K_a values for the different container·drug complexes translate into PSDs with different slopes. For example, a change in slope from 0.1 to 0.5 and from 0.5 to 0.9 each corresponds to a 9-fold increase of K_a. Importantly, a precise knowledge of S_0 is not necessary in order to calculate relative K_a values (K_{rel} = $K_{a,C1\cdot D1}/K_{a,C2\cdot D1}$) from the PSDs obtained with two different containers (e.g., C1 and C2) toward a common drug (e.g., D1) because the S_0 values cancel as shown in eq 2. If S_0 is known precisely, then absolute K_a

dx.doi.org/10.1021/jm501276u | J. Med. Chem. 2014, 57, 9554−9563

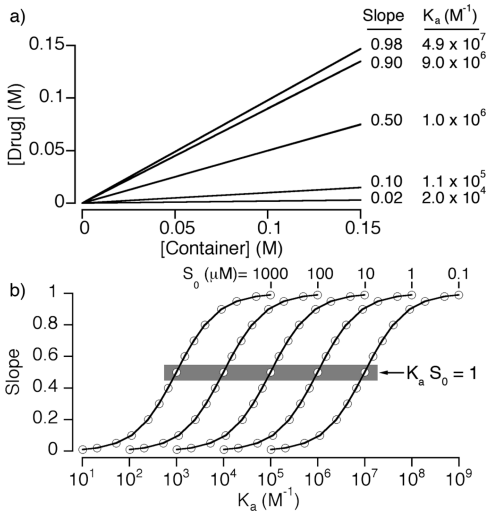

Figure 3. Simulations of the phase solubility behavior of hypothetical container·drug 1:1 systems that obey eq 1. (a) Plot of [Drug] versus [Container] for a system with S_0 = 1 μM and five different K_a values. (B) Plot of slope of the PSD versus K_a (M^{-1}) for five different values of S_0 (1 mM, 100 μM, 10 μM, 1 μM, 100 nM).

values can be calculated using eq 1. Figure 3b shows a plot of the slope of the PSD as a function of the K_a for the container·drug complex for five different values of S_0 (1 mM, 100 μM, 10 μM, 1 μM, 0.1 μM). Clearly, the lower the inherent solubility of the drug (S_0), the higher the value of K_a needed to result in a PSD of comparable slope. As a special case of eq 1, consider the situation when $(K_a)(S_0) = 1$; under this constraint, then slope = 0.5 (Figure 3b). From a practical point of view this means that to efficiently solubilize an insoluble drug (e.g., slope of PSD = 0.5) with an inherent solubility of 10 μM (100 nM) requires a K_a value of 10^5 M^{-1} (10^7 M^{-1}). In theory, the high values of K_a that are typically observed for CB[n]-type receptors promise to enable the solubilization of drugs whose solubilities are too low to be solubilized by lower affinity hosts (e.g., cyclodextrins).

$$K_a = \frac{\text{slope}}{S_0(1 - \text{slope})} \quad (1)$$

$$K_{rel} = \frac{K_{a,C1\cdot D1}}{K_{a,C2\cdot D1}} = \frac{\dfrac{\text{slope}_{C1\cdot D1}}{S_{0,D1}(1 - \text{slope}_{C1\cdot D1})}}{\dfrac{\text{slope}_{C2\cdot D1}}{S_{0,D1}(1 - \text{slope}_{C2\cdot D1})}} = \frac{(\text{slope}_{C1\cdot D1})(1 - \text{slope}_{C2\cdot D1})}{(\text{slope}_{C2\cdot D1})(1 - \text{slope}_{C1\cdot D1})} \quad (2)$$

Use of 1a−1e as Solubilizing Agents for Insoluble Drugs. In order to more fully understand the correlation between container structure (e.g., **1a−1e**), drug structure and properties, and the ability of the containers to solubilize insoluble drugs, we created PSDs for containers **1a−1e** and HP-β-CD with the 19 insoluble drugs (**8−26**) shown in Figure 2. Of these, 18 are drugs currently used in practice along with PBS-1086 (**17**) which is a developmental compound with documented anticancer activity.[18] To create these PSDs we stir an excess of insoluble drug with a known concentration of container until equilibrium is achieved, then remove remaining insoluble drug by filtration or centrifugation, and measure the concentration of drug in the supernatant by ^{1}H NMR spectroscopy. Our ^{1}H NMR assay relies on the addition of a known concentration of 1,3,5-benzene tricarboxylic acid as a nonbinding internal standard of known concentration which allows us to use the ratio of the integrals for drug versus internal standard to measure drug concentration. We have measured full PSDs for all 19 drugs with the six containers (Supporting Information). In nearly all cases, linear PSDs were observed at low [container] indicative of well-defined 1:1 complex formation, although some of the PSDs display plateau regions at higher [container] which indicates that the solubility of the container·drug complex is lower than that of the uncomplexed container. Table 1 gives the initial slopes of the PSDs determined by linear regression for all container−drug combinations. Table 1 also presents the K_{rel} values calculated using eq 2 referenced to the weakest binding host (usually HP-β-CD with K_{rel} = 1). The uncertainties in K_{rel} are generally ≈10−20%, although larger uncertainties are noted for PSDs with slope greater than 0.8. Figure 4 presents the PSDs measured for three drugs [estradiol (**18**), developmental anticancer agent **17**, camptothecin (**14**)] with the 6 different containers. In the sections below, we analyze the data presented in Table 1 to ascertain key features of the use of acyclic CB[n]-type containers as solubilizing excipients for insoluble drugs.

*Container **1b** Is the Most Potent Solubilizing Agent.* Of the 19 drugs tested, compound **1b** is the most efficient solubilizing agent (e.g., largest slope, highest K_{rel}) for 12 drugs, and is nearly the best for one additional drug [slopes for ziprasidone (**26**): **1b** = 0.432 versus **1e** = 0.458]. For five drugs [melphalan (**10**), amiodarone (**13**), camptothecin (**14**), 17α-ethynylestradiol (**19**), voriconazole (**24**)], **1b** forms such tight complexes (slope ≈1) that it is not possible to calculate a K_{rel} value using eq 1. Acyclic CB[n]-type containers including **1a** and **1b** are known to be relatively flexible[11f,19] and often exhibit an out-of-plane distortion (e.g., helical twist) as they wrap around their guests. Accordingly, each container·drug complex will exhibit a different geometry based on the size, shape, and functionality of the drug. However, we offer some rationale for the observed superior performance of **1b**. Figure 5 shows the previously reported X-ray structures of **1a** and **1b** as their CF_3CO_2H solvates.[11c] First, the size of the cavity of **1b** is larger than that of **1a** as measured by the distance between the opposing quaternary C atoms (**1a**, 10.93 and 11.44 Å; **1b**, 11.99 and 12.90 Å) of the dimethylglycoluril units. The increased size of **1b** is caused by its longer naphthalene sidewalls (relative to **1a**) which would clash sterically in a more compact geometry. Second, the naphthalene walls of **1b** engage in edge-to-face $\pi-\pi$ interactions with one another that creates a large hydrophobic π-surface that should allow it to simultaneously engage in edge-to-face and offset face-to-face $\pi-\pi$ interactions with insoluble aromatic drugs. Containers **1d** and **1e** which feature Me and cyclohexyl substituted *o*-xylylene sidewalls should possess larger cavities than **1a**; however, the alkyl substitution reduces the available π-surface area which should decrease their affinity toward insoluble aromatic compounds. For container **1c**, the isomeric naphthalene sidewalls are of comparable length to **1a** and result in a narrow and deep cavity. Accordingly, we surmise that the length of the naphthalene walls of **1b** and their ability to define a hydrophobic box of large π-surface area makes **1b** a superior solubilizing agent relative to containers **1a** and **1c−1e**.

Solubilization of Steroids. The test panel of insoluble drugs contained three steroids [estradiol (**18**), 17-α-ethynylestradiol (**19**), and fulvestrant (**25**)]. Steroids can often be solubilized with HP-β-CD, which allows a head-to-head comparison with

dx.doi.org/10.1021/jm501276u | J. Med. Chem. 2014, 57, 9554−9563

Table 1. Inherent Solubility (S_0, μM) of Selected Drugs and Values of Slope Calculated from the Linear Region of the PSDs for Containers 1a−1e and HP-β-CD with Drugs 8−26[a]

		1a		1b		1c	
	S_0 (μM)	slope	K_{rel} K_a	slope	K_{rel} K_a	slope	K_{rel} K_a
8	n.d.	n.l.	—	0	—	0	—
9	2.7 ± 0.34	0.12 ± 0.0041	9.4 ± 0.45 5.1(±0.67) × 10^4	0.48 ± 0.076	62 ± 13 3.4(±0.85) × 10^5	0.026 ± 0.0032	1.8 ± 0.23 1.0(±0.18) × 10^4
10	n.d.	1.2 ± 0.0080	TL	1.1 ± 0.072	TL	0.81 ± 0.10	34 ± 19
11	12 ± 1.9	0.040 ± 0.0031	1.5 ± 0.15 3.5(±0.62) × 10^3	0.10 ± 0.0071	3.9 ± 0.39 9.4(±1.6) × 10^3	0.46 ± 0.010	30 ± 2.2 7.2(±1.2) × 10^4
12	14 ± 1.7	0.59 ± 0.0095	6.3(±0.30) × 10^2 1.0(±0.14) × 10^5	0	— —	0	— —
13	66 ± 2.7	0.080 ± 0.0074	0.89 ± 0.11 1.3(±0.13) × 10^3	1.03 ± 0.15	TL TL	0.14 ± 0.0074	1.6 ± 0.18 2.4(±0.16) × 10^3
14	54 ± 3.9	0.14 ± 0.0070	1.0 ± 0.073 2.9(±0.26) × 10^3	1.1 ± 0.059	TL TL	0.26 ± 0.019	2.2 ± 0.20 6.3(±0.67) × 10^3
15	5.7 ± 1.1	0.024 ± 0.0017	1.8 ± 0.14 4.4(±0.90) × 10^3	0.47 ± 0.037	67 ± 7.3 1.6(±0.35) × 10^5	0.022 ± 0.0022	1.69 ± 0.17 4.0(±0.87) × 10^3
16	1.9 ± 0.41	0.043 ± 0.0037	5.8 ± 1.2 2.4(±0.55) × 10^4	0.54 ± 0.017	1.5(±0.30) × 10^2 6.3(±1.4) × 10^5	0.052 ± 0.0023	7.0 ± 1.4 2.9(±0.63) × 10^4
17	4.5 ± 0.90	0.71 ± 0.027	15 ± 2.0 5.5(±1.2) × 10^5	0.89 ± 0.0043	50 ± 5.0 1.9(±0.38) × 10^6	0.14 ± 0.013	1.0 3.7(±0.82) × 10^4
18	8.8 ± 0.42	0.35 ± 0.019	2.4 ± 0.15 6.2(±0.48) × 10^4	0.92 ± 0.053	51 ± 33 1.3(±0.86) × 10^6	0.38 ± 0.015	2.7 ± 0.14 7.0(±0.46) × 10^4
19	24 ± 2.4	0.35 ± 0.016	1.0 2.2(±0.24) × 10^4	1.1 ± 0.0045	TL TL	0.41 ± 0.071	1.25 ± 0.27 2.8(±0.65) × 10^4
20	n.d.	0	—	0	—	0.12 ± 0.0098	8.6 ± 1.8
21	23 ± 3.1	0.066 ± 0.0034	2.0 ± 0.16 3.1(±0.45) × 10^3	0.31 ± 0.027	13 ± 1.4 2.0(±0.32) × 10^4	0.034 ± 0.0020	1.0 1.5(±0.23) × 10^3
22	n.d.	0	—	n.l.	—	0	—
23	n.d.	0.079 ± 0.0092	1.0	0	—	0	—
24	38 ± 1.6	0.50 ± 0.047	3.4 ± 0.54 2.6(±0.36) × 10^4	1.0 ± 0.026	TL TL	0.40 ± 0.037	2.3 ± 0.32 1.7(±0.20) × 10^4
25	n.d.	0	—	0.10 ± 0.0055	1.0	0	—
26	63 ± 3.5	1.1 ± 0.19	TL	0.43 ± 0.052	29 ± 5.0 1.2(±0.2) × 10^4	0.18 ± 0.018	8.2 ± 1.1 3.4(±0.40) × 10^3

		1d		1e		HP-β-CD	
	S_0 (μM)	slope	K_{rel} K_a	slope	K_{rel} K_a	slope	K_{rel} K_a
8	n.d.	0	—	0	—	0	—
9	2.7 ± 0.34	0.10 ± 0.0057	8.0 ± 0.51 4.3(±0.60) × 10^4	0	— —	0.015 ± 0.0005	1.0 5.4(±0.71) × 10^3
10	n.d.	0.80 ± 0.071	32 ± 12	0.47 ± 0.053	6.9 ± 1.3	0.11 ± 0.012	1.0
11	12 ± 1.9	0.060 ± 0.0046	2.2 ± 0.23 5.4(±0.94) × 10^3	0	— —	0.028 ± 0.0019	1.0 2.4(±0.41) × 10^3
12	14 ± 1.7	0	— —	0.057 ± 0.0011	27 ± 1.1 4.4(±0.56) × 10^3	0.0020 ± 0.000086	1.0 1.6(±0.22) × 10^2
13	66 ± 2.7	0.13 ± 0.0039	1.5 ± 0.14 2.2(±0.11) × 10^3	0.13 ± 0.0050	1.6 ± 0.16 2.3(±0.13) × 10^3	0.089 ± 0.0083	1.0 1.5(±0.15) × 10^3
14	54 ± 3.9	0.50 ± 0.010	6.4 ± 0.38 1.9(±0.14) × 10^4	0.13 ± 0.0070	1.0 2.9(±0.26) × 10^3	0 0	— —
15	5.7 ± 1.1	0.017 ± 0.0018	1.3 ± 0.14 3.0(±0.67) × 10^3	0	— —	0.013 ± 0.00040	1.0 2.4(±0.46) × 10^3
16	1.9 ± 0.41	0.033 ± 0.0045	4.4 ± 1.0 1.9(±0.14) × 10^4	0	— —	0.0080 ± 0.0015	1.0 4.1(±1.2) × 10^3
17	4.5 ± 0.90	0.52 ± 0.023	6.4 ± 0.73 2.4(±0.51) × 10^5	0.16 ± 0.017	1.1 ± 0.16 4.2(±0.96) × 10^4	0 0	— —
18	8.8 ± 0.42	0.61 ± 0.056	6.8 ± 1.2 1.8(±0.31) × 10^5	0.52 ± 0.064	4.7 ± 0.86 1.2(±0.23) × 10^5	0.18 ± 0.0025	1.0 2.6(±0.13) × 10^4
19	24 ± 2.4	0.38 ± 0.026	1.1 ± 0.11 2.5(±0.32) × 10^4	0.44 ± 0.014	1.4 ± 0.094 3.2(±0.34) × 10^4	0.47 ± 0.048	1.62 ± 0.24 3.6(±0.61) × 10^4

dx.doi.org/10.1021/jm501276u | J. Med. Chem. 2014, 57, 9554−9563

Table 1. continued

		1d		1e		HP-β-CD	
	S_0 (μM)	slope	K_{rel} K_a	slope	K_{rel} K_a	slope	K_{rel} K_a
20	n.d.	0.016 ± 0.0030	1.0	0.021 ± 0.0017	1.3 ±	0	—
21	23 ± 3.1	0	—	0	—	0	—
22	n.d.	0	—	0	—	0	—
23	n.d.	0	—	0	—	0	—
24	38 ± 1.6	0.83 ± 0.063	17 ± 6.7 1.3(±0.51) × 10^5	0.87 ± 0.054	22 ± 9.3 1.7(±0.70) × 10^5	0.22 ± 0.018	1.0 7.6(±0.71) × 10^3
25	n.d.	0	—	0	—	0	—
26	63 ± 3.5	0.39 ± 0.013	24 ± 2.3 1.0(±0.069) × 10^4	0.46 ± 0.021	32 ± 3.3 1.4(±0.11) × 10^4	0.026 ± 0.0022	1.0 4.2(±0.43) × 10^2

[a]The corresponding K_a (M^{-1}) and K_{rel} values were calculated using eqs 1 and 2. n.d. = not determined, n.l. = nonlinear PSD; — = could not be determined because PSD is nonlinear or slope = 0; TL = too large to be determined from PSD.

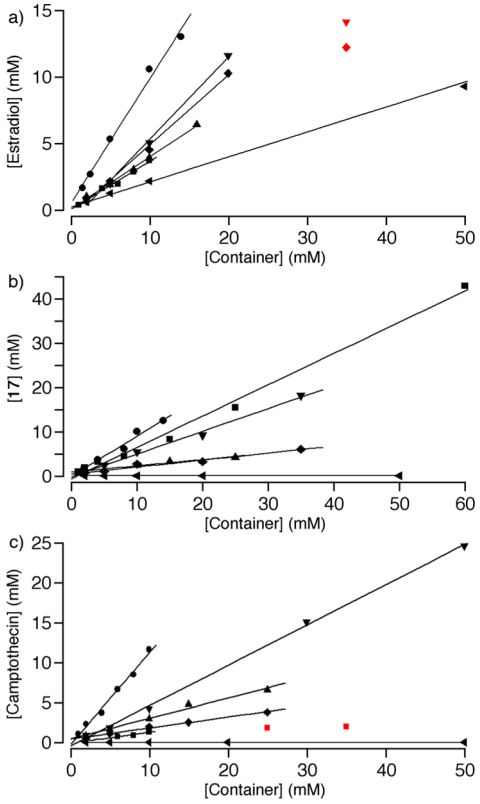

Figure 4. PSDs constructed for mixtures of containers (**1a**, ■; **1b**, ●; **1c**, ▲; **1d**, ▼; **1e**, ◆; HP-β-CD, ◀) with selected insoluble drugs: (a) estradiol (**18**), (b) **17**, (c) camptothecin (**14**). Conditions: 20 mM sodium phosphate buffered D_2O (pH = 7.4, rt). The red data points were not used in the linear regression.

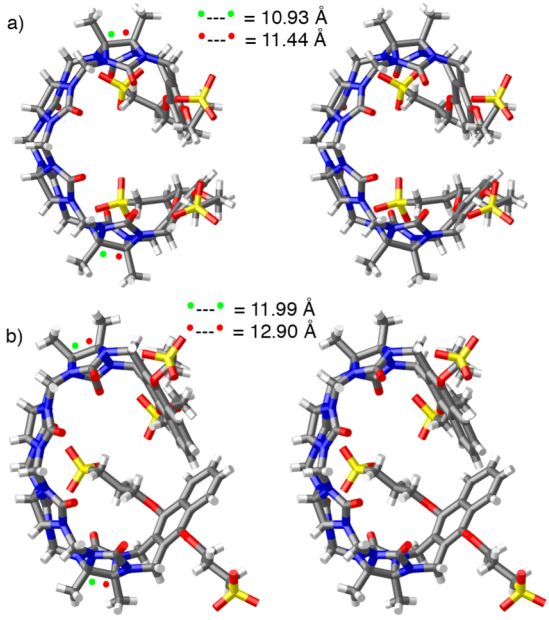

Figure 5. Cross-eyed stereoscopic representations of the X-ray crystal structures of (a) **1a** and (b) **1b**. Solvating CF_3CO_2H molecules have been omitted for clarity. Color code: C, gray; H, white; N, blue; O, red; S, yellow.

our acyclic CB[*n*]-type containers. Figure 4a shows the PSDs measured for all six containers toward estradiol (**18**) which is illustrative. All five acyclic CB[*n*]-type containers **1a**–**1e** solubilize estradiol more efficiently (slope = 0.35 to 0.92; K_{rel} from 2.4 to 51) than HP-β-CD (slope =0.18; K_{rel} = 1.0). Figure 6a–c shows the ^{1}H NMR spectra recorded for estradiol alone in DMSO-d_6 and in the presence of **1a** and **1b** in buffered D_2O. The large upfield shifts observed for the axial Me-group (H_k) and the protons on the sp^3-hydridized C atoms of the steroidal skeleton indicate that the containers bind preferentially to this region of the steroids. Container **1b** solubilizes 17-α-ethynylestradiol (**19**) with 1:1 stoichiometry which is indicative of a very large association constant K_a for this complex. Only container **1b** was capable of solubilizing fulvestrant (**25**) which is both highly hydrophobic and fluorinated. Previously, we have established that **1b** binds to the neuromuscular blocking agents rocuronium and vecuronium which are steroidal diammoniums with $K_a > 10^9$ M^{-1}.[11d] In combination, these results allow us to conclude that acyclic CB[*n*]-type containers (but especially **1b**) are better receptors for steroids than HP-β-CD.

Developmental Anticancer Agent ***17***. Compound **17** is a developmental drug with documented *in vivo* anticancer activity using a DMSO formulation, but which could not be formulated in water using the standard techniques including cyclodextrins.[18a] Accordingly, we decided to investigate the formulation of **17** using containers **1a**–**1e** (Table 1 and Figure 4b). All five acyclic CB[*n*]-type containers solubilize **17** (slope = 0.14–0.89) whereas HP-β-CD is incapable of solubilizing this drug. Interestingly, although **17** is most efficiently solubilized by **1b** (slope = 0.89), container **1a** (slope = 0.71) generates a solution with the highest concentration of **17** because of the higher inherent solubility of **1a**. Compound **17** is also nicely solubilized by **1d** which is perhaps unsurprising given that the

dx.doi.org/10.1021/jm501276u | J. Med. Chem. 2014, 57, 9554–9563

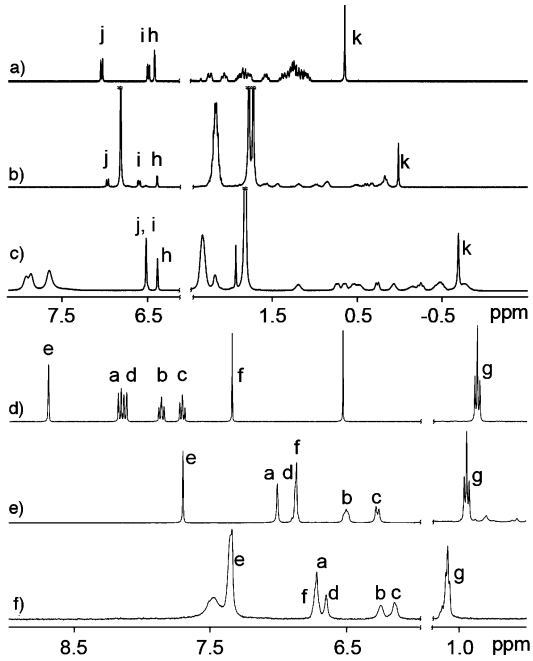

Figure 6. ^{1}H NMR recorded (400 MHz, rt, 20 mM sodium phosphate buffered D_2O, pH 7.4) for (a) estradiol **18** (in DMSO-d_6), (b) **1a** (10 mM) with estradiol **18**, (c) **1b** (10 mM) with estradiol **18**, (d) camptothecin **14** (in DMSO-d_6), (e) **1d** (15 mM) with camptothecin **14**, and (f) **1b** (10 mM) with camptothecin **14**.

Me-substituted sidewalls of **1d** makes it intermediate in size (Figure 5) between **1a** and **1b**.

Acyclic CB[n]-type Containers Are Good Solubilizing Agents for Insoluble Drugs Containing Aromatic Rings. The X-ray crystal structures of **1a** and **1b** (Figure 5) show that the aromatic sidewalls are oriented roughly perpendicular to one another and define a hydrophobic box. Accordingly, it would be expected that insoluble drugs that contain aromatic rings would be good guests for acyclic CB[*n*]-type containers. The majority of drugs studied in this paper contain aromatic rings within their structure, and we generally observed upfield shifting of the ^{1}H NMR resonances of these aromatic rings upon complexation with **1a**−**1e**. Those aromatic rings with attached ammonium functional groups (e.g., anilines, benzimidazoles, *N*-arylpiperazines) constitute preferred binding sites. In only one case (amiodarone, **13**) was complexation at an aliphatic ammonium (Pr_2NHR^+) moiety predominant. The observed upfield shifting of the aromatic protons confirms that the aromatic residues of the drugs are encapsulated within the hydrophobic box that is defined by the two aromatic walls and the methylene bridged glycoluril tetramer backbone. For example, Figure 6d−f shows the ^{1}H NMR spectra recorded for camptothecin (**14**) alone in DMSO-d_6 and in water in the presence of containers **1d** and **1b**. Obviously, the protons on the aromatic rings of camptothecin (H_a−H_f) undergo substantial upfield shifts upon complexation. Larger upfield shifts are observed upon complexation with **1b** probably because of the larger anisotropic shielding effect of the naphthalene walls of **1b** relative to the *o*-xylylene walls of **1d**. Figure 4c shows the PSDs created for mixtures of camptothecin (**14**) with containers **1a**−**1e** and HP-*β*-CD which display A_L-type PSDs indicative of 1:1 complexation. All five acyclic CB[*n*]-type containers (**1a**−**1e**) solubilize camptothecin (**14**) nicely, with **1b** doing so in equimolar amounts whereas HP-*β*-CD is unable to solubilize camptothecin under these conditions. Among containers **1a**−**1e**, container **1e** displays the narrowest scope of solubilizing abilities with 9 out of 19 drugs displaying no solubilization. We attribute the poor solubilization abilities of **1e** to the half-chair conformation of its tetrahydronaphthalene walls which sterically impede π−π interactions. We believe that the strategic merging of the structural features of CB[*n*] receptors (to deliver strong hydrophobic binding and ammonium binding) with the aromatic walls of cyclophanes to impart affinity toward the wide variety of insoluble aromatic drugs positions acyclic CB[*n*]-type receptors as a powerful alternative to cyclodextrins that expands the scope of insoluble drugs that can be formulated with molecular container technology.

Some Drugs Are Solubilized by a Narrow Set of Containers. Four drugs are solubilized by only one acyclic CB[*n*]-type container: paclitaxel (**8**) and docetaxel (**23**) by **1a**, fenofibrate (**22**) and fulvestrant (**25**) by **1b**. Cinnarizine (**12**) is only solubilized by two containers; it is best solubilized by **1a** and less well by **1e**. On the basis of this data we believe that containers **1a** and **1b** are the most versatile and general purpose solubilizing agents and that these containers are best positioned for further development as novel solubilizing excipients for practical applications.

*Container **1d** Is Structurally and Functionally Intermediate between **1a** and **1b**.* The dimethyl substituted *o*-xylylene walls of container **1d** are intermediate in length between **1a** and **1b** which feature benzene and napthalene derived sidewalls. Compound **1d** is also intermediate between **1a** and **1b** in terms of its self-association properties but possesses superior solubility characteristics (353 mM) in buffered water. Accordingly, and perhaps unsurprisingly, we find that **1d** exhibits solubilization abilities that are similar to those of **1a** and **1b**. For example, for albendazole (**9**), melphalan (**10**), amiodarone (**13**), indomethacin (**15**), and tolfenamic acid (**16**), the slopes and K_{rel} values for **1d** are comparable to those of **1a** but significantly smaller than the corresponding values measured for **1b**. For other drugs, namely voriconazole (**24**) and ziprasidone (**26**), the slope and K_{rel} values measured for **1d** are more comparable to those of **1b** than **1a**.

Comparison of the Binding Affinity of 1a−1e with HP-*β*-CD toward Insoluble Drugs. It is also possible to determine the absolute K_a value for container·drug complexes from the PSDs if the solubility of the uncomplexed drug (S_0) is known. Accordingly, we measured the inherent solubility for 13 of the 19 drugs studied and used these S_0 values to determine the absolute K_a values for this selection of drugs as given in Table 1. The binding constants for these 13 drugs toward HP-*β*-CD span the range 160−36 000 M^{-1} which is in line with the well-known low affinity (log K_a = 2.5 ± 1.1 M^{-1}) and low selectivity of cyclodextrins toward their guests.[20] In contrast, the K_a values measured for these 13 drugs toward **1a**−**1e** fall in the range 1300 to 1.9 × 10^6 M^{-1} with three additional complexes too tight to measure using the PSD. For drugs that are solubilized by HP-*β*-CD, the best acyclic container (e.g., **1a**−**1e**) always forms significantly stronger container·drug complexes (29- to 630-fold stronger) than HP-*β*-CD. In many cases the acyclic containers bind to and solubilize drugs [e.g., camptothecin (**14**) and aripiprazole (**21**)] that cannot be solubilized at all with HP-*β*-CD under these conditions. The ability of **1a**−**1e** to solubilize drugs that cannot be solubilized with HP-*β*-CD and to do so more efficiently (larger slope and

dx.doi.org/10.1021/jm501276u | J. Med. Chem. 2014, 57, 9554−9563

K_a) suggests that acyclic CB[n]-type containers will become an important tool to formulate insoluble pharmaceutical agents.

CONCLUSIONS

In summary, we have compared the ability of **1a**−**1e** to solubilize insoluble drugs relative to HP-β-CD. Compounds **1a**−**1e** do not undergo strong self-association ($K_s \leq 624$ M^{-1}) in buffered water and possess good solubility characteristics. We created PSDs for mixtures of containers **1a**−**1e** and HP-β-CD with 19 drugs. We find that the solubilizing ability of the best container (**1a**−**1e**) is superior to HP-β-CD in all cases; **1a**−**1e** even solubilize 8 drugs that are completely insoluble with HP-β-CD. The superior solubilizing ability can be traced to the 29- to 630-fold higher binding affinity of the best acyclic CB[n]-type container toward the drugs compared to HP-β-CD. Less container is needed, therefore, to achieve a given [drug]. A notable achievement was the solubilization of the developmental anticancer agent **17**. The acyclic CB[n]-type containers display an affinity for the steroid ring system, aromatic moieties of insoluble drugs, and cationic ammonium groups. Compound **1b** is generally the most potent (K_a up to and exceeding 10^6 M^{-1}) container whereas both **1a** and **1b** display excellent solubility enhancement toward a broad range of insoluble drugs. The broad scope of insoluble drugs that can be formulated with **1a** and **1b**, in many cases where HP-β-CD fails completely, makes acyclic CB[n]-type containers particularly attractive alternatives to cyclodextrins as solubilizing excipients for practical applications.

EXPERIMENTAL SECTION

General Experimental. Starting materials were purchased from commercial suppliers and were used without further purification. Compounds **1a**−**1c**, **2**, **5**, and **6** were prepared according to literature procedures.[11b,c,e,13] Melting points were measured on a Meltemp apparatus in open capillary tubes and are uncorrected. IR spectra were measured on a JASCO FT/IR 4100 spectrometer by attenuated total reflectance (ATR) and are reported in cm^{-1}. NMR spectra were measured at 400 or 600 MHz for ^1H and 125 MHz for ^{13}C. Integration of the ^1H NMR spectra indicates that the new compounds have a level of purity ≥95%. Mass spectrometry was performed using a JEOL AccuTOF electrospray instrument using the electrospray ionization technique.

*1-Propanesulfonic Acid, 2,3,15,16-Tetramethyl-3,3′,3″,3‴-[[(19bα,19cα,21bα,21cα,23bα,23cα,25bα,25cα)-5,13,18,19b,19c,21b,21c,23b,23c,25b,25c,26-dodecahydro-19b,19c,25b,25c-tetramethyl-6,8,10,12,19,21,23,25-octaoxo-6H,7H,8H,9H,10H,11H,12H,19H,20H,21H,22H,23H,24H,25H-5a,6a,7a,8a,9a,10a,11a,12a,18a,19a,20a,21a,22a,23a,24a,25a-hexadecaazabisbenzo[5″,6″]cyclohepta[1″,2″,3″:3′,4′]pentaleno[1′,6′:5,6,7]cycloocta[1,2,3-gh:1′,2′,3′-g′h′]cycloocta[1,2,3-cd:5,6,7-c′d′]dipentalene-1,4,14,17-tetrayl]tetrakis(oxy)]tetrakis-, Sodium Salt (1:4) (**1d**).* Compound **3d** (0.65 g, 1.5 mmol) was added into a solution of **2** (0.30 g, 0.38 mmol) in TFA/Ac_2O (3.0 mL, v/v = 1:1). The mixture was stirred and heated at 70 °C for 3 h. The solvent was removed under reduced pressure, and the solid was dried under high vacuum. The solid was recrystallized from a mixture of water and EtOH (1:2, v/v, 20 mL) twice and then dissolved in water and adjusted to pH = 7 with 1 M aqueous NaOH. The solvent was removed under reduced pressure. The resulting solid was dried under high vacuum to yield **1d** as a white solid (0.26 g, 43%). Mp >300 °C. IR (ATR, cm^{-1}): 2999w, 2952w, 2875w, 1733s, 1652s, 1474s, 1368m, 1321m, 1233s, 1185s, 1093m, 1044s, 960w, 823w, 800m, 795m. ^1H NMR (400 MHz, D_2O): δ 5.68 (d, J = 15.3, 2H), 5.59 (d, J = 15.7, 4H), 5.43 (d, J = 7.8, 2H), 5.36 (d, J = 7.8, 2H), 5.17 (d, J = 16.1, 4H), 4.35 (d, J = 16.1, 4H), 4.25 (d, J = 15.7, 4H), 4.07 (d, J = 15.3, 2H), 4.00−3.80 (m, 4H), 3.75−3.55 (m, 4H), 3.25−3.05 (m, 8H), 2.25−2.15 (m, 8H), 1.82 (s, 12H), 1.78 (s, 6H), 1.74 (s, 6H). ^{13}C NMR (125 MHz, D_2O, 1,4-dioxane as internal reference): δ 156.1, 155.5, 149.7, 130.9, 127.6, 78.0, 76.9, 72.1, 70.7, 70.5, 52.1, 47.8, 47.3, 35.6, 24.3, 15.8, 14.8, 11.8. HR-MS (ESI): m/z 753.1997 ($[M - 4Na + 2H]^{2-}$, $C_{58}H_{74}N_{16}O_{24}S_4$, calcd for 753.1972).

*1-Propanesulfonic Acid, 3,3′,3″,3‴-[[(22bα,22cα,24bα,24cα,26bα,26cα,28bα,28cα)-6, 14,21,22b,22c,24b,24c,26b,26c,28b,28c,29-dodecahydro-22b,22c,28b,28c-tetramethyl-7,9,11,13,22,24,26,28-octaoxo-7H,8H,9H,10H,11H,12H,13H,22H,23H,24H,25H,26H,27H,28H-6a,7a,8a,9a,10a,11a,12a,13a,21a,22a,23a,24a,25a,26a,27a,28a-hexadecaazacyclooctа[1,2,3:3″,4″;5,6,7:3‴,4‴]dipentaleno[1″,6″:5,6,7:1‴,6‴:5′,6′,7′]dicycloocta[1,2,3:3″,4″;1′,2′,3′:3‴,4‴]dipentaleno[1″,6″:4,5,6;1‴,6‴:4′,5′,6′]dicyclohepta[1,2-b:1′,2′-b′]di-5,6,7,8-tetrahydronaphthalene-5,15,20,30-tetrayl]tetrakis(oxy)]-tetrakis-, Sodium Salt (1:4) (**1e**).* Compound **3e** (1.1 g, 2.5 mmol) was added into a solution of **2** (0.50 g, 0.64 mmol) in TFA/Ac_2O (5.0 mL, v:v = 1:1). The mixture was stirred and heated at 70 °C for 3 h. The solvent was removed under reduced pressure, and the solid was dried under high vacuum. The solid was recrystallized from a mixture of water and EtOH (1:2, v/v, 0.30 L) twice and then dissolved in water and adjusted to pH = 7 by adding 1 M aqueous NaOH. The solvent was removed under reduced pressure, and the solid was dried under high vacuum to yield **1e** as a white solid (0.30 g, 30%). Mp >300 °C. IR (ATR, cm^{-1}): 2930w, 2875w, 1724s, 1471s, 1375m, 1320m, 1233s, 1171s, 1084m, 1041s, 824w, 801m, 759w. ^1H NMR (400 MHz, D_2O, with added *p*-xylenediamine): δ 5.64 (d, J = 15.8, 4H), 5.49 (d, J = 15.5, 2H), 5.45 (d, J = 8.8, 2H), 5.28 (d, J = 8.8, 2H), 5.23 (d, J = 16.4, 4H), 4.38 (d, J = 16.4, 4H), 4.29 (d, J = 15.8, 4H), 3.97 (d, J = 15.5, 2H), 4.00−3.80 (m, 4H), 3.75−3.65 (m, 4H), 3.25−3.15 (m, 8H), 2.65−2.50 (m, 4H), 2.30−2.15 (m, 12H), 1.88 (s, 6H), 1.83 (s, 6H), 1.60−1.55 (m, 4H), 1.35−1.20 (m, 4H). ^{13}C NMR (125 MHz, D_2O, with added *p*-xylenediamine and 1,4-dioxane as internal reference): δ 156.5, 155,7, 149.7, 132.0, 131.6, 127.8, 126.7, 78.3, 77.2, 71.7, 71.2, 71.0, 52.7, 48.4, 47.6, 41.6, 35.6, 24.7, 22.9, 21.0, 15.5, 14.8. HR-MS (ESI): 779.2154 ($[M - 4Na + 2H]^{2-}$, $C_{62}H_{78}N_{16}O_{24}S_4$, calcd for 779.2129).

*Sodium 3,3′-((2,3-dimethyl-1,4-phenylene)bis(oxy))bis(propane-1-sulfonate) (**3d**).* A solution of **4** (18 g, 0.15 mol) in 1,4-dioxane (130 mL) was added into a solution of 2,3-dimethylhydroquinone (8.0 g, 58 mmol) in aqueous NaOH solution (1.0 M, 0.10 L). The mixture was stirred at rt for 12 h and then filtered to collect the crude solid. The solid was stirred with acetone (0.20 L) and then dried under high vacuum to yield **3d** as a pale red solid (18 g, 73%). Mp >280 °C. IR (ATR, cm^{-1}): 2938w, 2869w, 1625m, 1489m, 1472m, 1205s, 1157s, 1112s, 1059s, 801m, 624m, 551m. ^1H NMR (400 MHz, D_2O): δ 6.88 (s, 2H), 4.10 (t, J = 5.6, 4H), 3.10 (t, J = 7.2, 4H), 2.15−2.05 (m, 8H), 1.71 (s, 6H). ^{13}C NMR (125 MHz, D_2O, 1, 4-dioxane as internal reference): δ 150.5, 127.6, 111.8, 68.2, 47.6, 24.1, 11.1. HR-MS (ESI): m/z 381.0694 ($[M - 2Na + H]^-$, $C_{14}H_{21}O_8S_2$, calcd for 381.0678).

*Sodium 3,3′-((5,6,7,8-tetrahydronaphthalene-1,4-diyl)bis(oxy))-bis(propane-1-sulfonate) (**3e**).* A solution of **4** (8.6 g, 70.0 mmol) in 1,4-dioxane (60 mL) was added to a solution of **7** (4.0 g, 28 mmol) in aqueous NaOH solution (1.0 M, 45 mL). The mixture was stirred at rt for 12 h and then filtered to collect the crude solid. The crude solid was stirred with acetone (0.10 L), filtered, and then dried under high vacuum to yield **3e** as a white solid (7.6 g, 60%). Mp >280 °C. IR (ATR, cm^{-1}): 2946w, 2846w, 1652w, 1471w, 1256m, 1194s, 1094m, 1045s, 791w, 604w, 521w. ^1H NMR (400 MHz, D_2O): δ 6.83 (s, 2H), 4.09 (t, J = 6.0, 4H), 3.08 (t, J = 6.2, 4H), 2.65−2.55 (m, 4H), 2.35−2.15 (m, 4H), 1.75−1.60 (m, 4H). ^{13}C NMR (125 MHz, D_2O, 1, 4-dioxane as internal reference): δ 150.0, 128.1, 110.2, 67.4, 47.6, 24.0, 22.7, 21.2. HR-MS (ESI): m/z 407.0842 ($[M - 2Na + H]^-$, $C_{16}H_{23}O_8S_2$, calcd for 407.0834).

*5,6,7,8-Tetrahydronaphthalene-1,4-diol (**7**).* A solution of **6** (5.3 g, 33 mmol) in EtOH (0.16 L) was mixed with palladium on activated carbon (3.5 g, 10 wt %, 3.3 mmol). The mixture was stirred under H_2 gas (15 Psi) for 3 days at rt. The heterogeneous reaction mixture was filtered, and the filtrate was concentrated under reduced pressure. After the residual solvent was removed under high vacuum, the product was obtained as a light purple solid (4.57 g, 85%). Characterization data matches the literature report.[14]

dx.doi.org/10.1021/jm501276u | J. Med. Chem. 2014, 57, 9554−9563

■ ASSOCIATED CONTENT

Supporting Information

^{1}H and ^{13}C NMR spectra for all new compounds, ^{1}H NMR self-association study data, procedures for solubility determination, phase solubility data and diagrams, and selected ^{1}H NMR spectra from the phase solubility measurements. This material is available free of charge via the Internet at http://pubs.acs.org.

■ AUTHOR INFORMATION

Corresponding Author

*E-mail: LIsaacs@umd.edu. Phone: 301-405-1884. Fax: 301-314-9121.

Notes

The authors declare no competing financial interest.

■ ACKNOWLEDGMENTS

We thank the National Cancer Institute of the National Institutes of Health (R01-CA168365) for financial support. B.Z. thanks the University of Maryland for a Wylie Dissertation fellowship. We thank Timothy Fouts, Jeffrey Meshulam, and Kathryn Bobb (Rel-MD) for samples of **17**.

■ ABBREVIATIONS USED

CB[*n*], cucurbit[*n*]uril; HP-*β*-CD, hydroxypropyl-*β*-cyclodextrin; K_a, binding constant; K_{rel}, relative binding constant; K_s, self-association constant; SBE-*β*-CD, sulfobutyl ether-*β*-cyclodextrin; *π*−*π*, pi−pi; PSD, phase solubility diagram; A_L-type, linear PSD; S_0, inherent drug solubility; ATR, attenuated total reflectance; s, strong IR signal; m, medium IR signal; w, weak IR signal

■ REFERENCES

(1) (a) Pedersen, C. J. The discovery of crown ethers (nobel lecture). *Angew. Chem., Int. Ed.* **1988**, *27*, 1021−1027. (b) Lehn, J.-M. Supramolecular chemistry—scope and perspectives: Molecules, supermolecules, and molecular devices. *Angew. Chem., Int. Ed.* **1988**, *27*, 89−112. (c) Cram, D. J. The design of molecular hosts, guests, and their complexes. *Angew. Chem., Int. Ed.* **1988**, *27*, 1009−1020. (d) Gutsche, C. D. Calixarenes. *Acc. Chem. Res.* **1983**, *16*, 161−170. (e) Diederich, F. Complexation of neutral molecules by cyclophane hosts. *Angew. Chem., Int. Ed.* **1988**, *27*, 362−386. (f) Yoshizawa, M.; Klosterman, J.; Fujita, M. Functional molecular flasks: New properties and reactions within discrete, self-assembled hosts. *Angew. Chem., Int. Ed.* **2009**, *48*, 3418−3438. (g) Rebek, J. Molecular behavior in small spaces. *Acc. Chem. Res.* **2009**, *42*, 1660−1668. (h) Lin, Z.; Emge, T. J.; Warmuth, R. Multicomponent assembly of cavitand-based polyacylhydrazone nanocapsules. *Chem.—Eur. J.* **2011**, *17*, 9395−9405.

(2) (a) Mal, P.; Breiner, B.; Rissanen, K.; Nitschke, J. R. White phosphorus is air-stable within a self-assembled tetrahedral capsule. *Science* **2009**, *324*, 1697−1699. (b) Trinh, T.; Cappel, J. P.; Geis, P. A.; McCarty, M. L.; Pilosof, D.; Zwerdling, S. S. (Procter and Gamble Company, USA). Uncomplexed cyclodextrin solutions for odor control on inanimate surfaces, especially fabrics. WO9605358A1, 1996. (c) Fiedler, D.; Leung, D. H.; Bergman, R. G.; Raymond, K. N. Selective molecular recognition, C-H bond activation, and catalysis in nanoscale reaction vessels. *Acc. Chem. Res.* **2005**, *38*, 349−358. (d) Kay, E. R.; Leigh, D. A.; Zerbetto, F. Synthetic molecular motors and mechanical machines. *Angew. Chem., Int. Ed.* **2007**, *46*, 72−191. (e) Yau, C. M. S.; Pascu, S. I.; Odom, S. A.; Warren, J. E.; Klotz, E. J. F.; Frampton, M. J.; Williams, C. C.; Coropceanu, V.; Kuimova, M. K.; Phillips, D.; Barlow, S.; Bredas, J.-L.; Marder, S. R.; Millar, V.; Anderson, H. L. Stabilisation of a heptamethine cyanine dye by rotaxane encapsulation. *Chem. Commun.* **2008**, 2897−2899. (f) Guo, D.-S.; Liu, Y. Supramolecular chemistry of p-sulfonatocalix[n]arenes and its biological applications. *Acc. Chem. Res.* **2014**, *47*, 1925−1934.

(3) (a) Lagona, J.; Mukhopadhyay, P.; Chakrabarti, S.; Isaacs, L. The cucurbit[n]uril family. *Angew. Chem., Int. Ed.* **2005**, *44*, 4844−4870. (b) Lee, J. W.; Samal, S.; Selvapalam, N.; Kim, H.-J.; Kim, K. Cucurbituril homologues and derivatives: New opportunities in supramolecular chemistry. *Acc. Chem. Res.* **2003**, *36*, 621−630. (c) Masson, E.; Ling, X.; Joseph, R.; Kyeremeh-Mensah, L.; Lu, X. Cucurbituril chemistry: A tale of supramolecular success. *RSC Adv.* **2012**, *2*, 1213−1247. (d) Nau, W. M.; Florea, M.; Assaf, K. I. Deep inside cucurbiturils: Physical properties and volumes of their inner cavity determine the hydrophobic driving force for host-guest complexation. *Isr. J. Chem.* **2011**, *51*, 559−577.

(4) (a) Liu, S.; Ruspic, C.; Mukhopadhyay, P.; Chakrabarti, S.; Zavalij, P. Y.; Isaacs, L. The cucurbit[n]uril family: Prime components for self-sorting systems. *J. Am. Chem. Soc.* **2005**, *127*, 15959−15967. (b) Rekharsky, M. V.; Mori, T.; Yang, C.; Ko, Y. H.; Selvapalam, N.; Kim, H.; Sobransingh, D.; Kaifer, A. E.; Liu, S.; Isaacs, L.; Chen, W.; Moghaddam, S.; Gilson, M. K.; Kim, K.; Inoue, Y. A synthetic host-guest system achieves avidin-biotin affinity by overcoming enthalpy-entropy compensation. *Proc. Natl. Acad. Sci. U. S. A.* **2007**, *104*, 20737−20742. (c) Cao, L.; Sekutor, M.; Zavalij, P. Y.; Mlinaric-Majerski, K.; Glaser, R.; Isaacs, L. Cucurbit[7]uril guest pair with an attomolar dissociation constant. *Angew. Chem., Int. Ed.* **2014**, *53*, 988−993. (d) Isaacs, L. Stimuli responsive systems constructed using cucurbit[n]uril-type molecular containers. *Acc. Chem. Res.* **2014**, *47*, 2052−2062. (e) Ko, Y. H.; Kim, E.; Hwang, I.; Kim, K. Supramolecular assemblies built with host-stabilized charge-transfer interactions. *Chem. Commun.* **2007**, 1305−1315. (f) Yang, H.; Yuan, B.; Zhang, X.; Scherman, O. A. Supramolecular chemistry at interfaces: Host-guest interactions for fabricating multifunctional biointerfaces. *Acc. Chem. Res.* **2014**, 2106−2115.

(5) (a) Lee, D.-W.; Park, K.; Banerjee, M.; Ha, S.; Lee, T.; Suh, K.; Paul, S.; Jung, H.; Kim, J.; Selvapalam, N.; Ryu, S.; Kim, K. Supramolecular fishing for plasma membrane proteins using an ultrastable synthetic host-guest binding pair. *Nat. Chem.* **2011**, *3*, 154−159. (b) Kasera, S.; Biedermann, F.; Baumberg, J. J.; Scherman, O. A.; Mahajan, S. Quantitative sers using the sequestration of small molecules inside precise plasmonic nanoconstructs. *Nano Lett.* **2012**, *12*, 5924−5928. (c) Ahn, Y.; Jang, Y.; Selvapalam, N.; Yun, G.; Kim, K. Supramolecular velcro for reversible underwater adhesion. *Angew. Chem., Int. Ed.* **2013**, *52*, 3140−3144. (d) Ghale, G.; Lanctot, A. G.; Kreissl, H. T.; Jacob, M. H.; Weingart, H.; Winterhalter, M.; Nau, W. M. Chemosensing ensembles for monitoring biomembrane transport in real time. *Angew. Chem., Int. Ed.* **2014**, *53*, 2762−2765.

(6) (a) Lipinski, C. A. Drug-like properties and the causes of poor solubility and poor permeability. *J. Pharmacol. Toxicol. Methods* **2000**, *44*, 235−249. (b) Hauss, D. J. Oral lipid-based formulations. *Adv. Drug Delivery Rev.* **2007**, *59*, 667−676.

(7) (a) Leuner, C.; Dressman, J. Improving drug solubility for oral delivery using solid dispersions. *Eur. J. Pharm. Biopharm.* **2000**, *50*, 47−60. (b) Muller, R. H.; Keck, C. M. Challenges and solutions for the delivery of biotech drugs—a review of drug nanocrystal technology and lipid nanoparticles. *J. Biotechnol.* **2004**, *113*, 151−170. (c) Serajuddin, A. T. M. Salt formation to improve drug solubility. *Adv. Drug Delivery Rev.* **2007**, *59*, 603−616. (d) Stella, V. J.; Nti-Addae, K. W. Prodrug strategies to overcome poor water solubility. *Adv. Drug Delivery Rev.* **2007**, *59*, 677−694.

(8) (a) Okimoto, K.; Rajewski, R. A.; Uekama, K.; Jona, J. A.; Stella, V. J. The interaction of charged and uncharged drugs with neutral (hp-beta-cd) and anionically charged (sbe7-beta-cd) beta-cyclodextrins. *Pharm. Res.* **1996**, *13*, 256−264. (b) Rajewski, R. A.; Stella, V. J. Pharmaceutical applications of cyclodextrins. 2. In vivo drug delivery. *J. Pharm. Sci.* **1996**, *85*, 1142−1169.

(9) (a) Dong, N.; Xue, S.-F.; Zhu, Q.-J.; Tao, Z.; Zhao, Y.; Yang, L.-X. Cucurbit[n]urils (n = 7, 8) binding of camptothecin and the effects on solubility and reactivity of the anticancer drug. *Supramol. Chem.* **2008**, *20*, 659−665. (b) Zhao, Y.; Buck, D. P.; Morris, D. L.; Pourgholami, M. H.; Day, A. I.; Collins, J. G. Solubilisation and

cytotoxicity of albendazole encapsulated in cucurbit[n]uril. *Org. Biomol. Chem.* **2008**, *6*, 4509−4515. (c) Zhao, Y.; Pourgholami, M. H.; Morris, D. L.; Collins, J. G.; Day, A. I. Enhanced cytotoxicity of benzimidazole carbamate derivatives and solubilisation by encapsulation in cucurbit[n]uril. *Org. Biomol. Chem.* **2010**, *8*, 3328−3337. (d) Dong, N.; Wang, X.; Pan, J.; Tao, Z. Influence of cucurbit(n=7,8)uril on the solubility and stability of chlorambucil. *Acta Chim. Sin.* **2011**, *69*, 1431−1437. (e) Jeon, Y. J.; Kim, S.-Y.; Ko, Y. H.; Sakamoto, S.; Yamaguchi, K.; Kim, K. Novel molecular drug carrier: Encapsulation of oxaliplatin in cucurbit[7]uril and its effects on stability and reactivity of the drug. *Org. Biomol. Chem.* **2005**, *3*, 2122−2125. (f) Miskolczy, Z.; Megyesi, M.; Tarkanyi, G.; Mizsei, R.; Biczok, L. Inclusion complex formation of sanguinarine alkaloid with cucurbit[7]uril: Inhibition of nucleophilic attack and photooxidation. *Org. Biomol. Chem.* **2011**, *9*, 1061−1070. (g) Kim, E.; Kim, D.; Jung, H.; Lee, J.; Paul, S.; Selvapalam, N.; Yang, Y.; Lim, N.; Park, C. G.; Kim, K. Facile, template-free synthesis of stimuli-responsive polymer nanocapsules for targeted drug delivery. *Angew. Chem., Int. Ed.* **2010**, *49*, 4405−4408. (h) Cao, L.; Hettiarachchi, G.; Briken, V.; Isaacs, L. Cucurbit[7]uril containers for targeted delivery of oxaliplatin to cancer cells. *Angew. Chem., Int. Ed.* **2013**, *52*, 12033−12037.

(10) (a) Chakraborty, A.; Wu, A.; Witt, D.; Lagona, J.; Fettinger, J. C.; Isaacs, L. Diastereoselective formation of glycoluril dimers: Isomerization mechanism and implications for cucurbit[n]uril synthesis. *J. Am. Chem. Soc.* **2002**, *124*, 8297−8306. (b) Huang, W.-H.; Liu, S.; Zavalij, P. Y.; Isaacs, L. Nor-seco-cucurbit[10]uril exhibits homotropic allosterism. *J. Am. Chem. Soc.* **2006**, *128*, 14744−14745. (c) Huang, W.-H.; Zavalij, P. Y.; Isaacs, L. Chiral recognition inside a chiral cucurbituril. *Angew. Chem., Int. Ed.* **2007**, *46*, 7425−7427. (d) Huang, W.-H.; Zavalij, P. Y.; Isaacs, L. Folding of long-chain alkanediammonium ions promoted by a cucurbituril derivative. *Org. Lett.* **2008**, *10*, 2577−2580. (e) Huang, W.-H.; Zavalij, P. Y.; Isaacs, L. Metal-ion-induced folding and dimerization of a glycoluril decamer in water. *Org. Lett.* **2009**, *11*, 3918−3921. (f) Lucas, D.; Minami, T.; Iannuzzi, G.; Cao, L.; Wittenberg, J. B.; Anzenbacher, P.; Isaacs, L. Templated synthesis of glycoluril hexamer and monofunctionalized cucurbit[6]uril derivatives. *J. Am. Chem. Soc.* **2011**, *133*, 17966−17976. (g) Vinciguerra, B.; Cao, L.; Cannon, J. R.; Zavalij, P. Y.; Fenselau, C.; Isaacs, L. Synthesis and self-assembly processes of monofunctionalized cucurbit[7]uril. *J. Am. Chem. Soc.* **2012**, *134*, 13133−13140.

(11) (a) Lucas, D.; Isaacs, L. Recognition properties of acyclic glycoluril oligomers. *Org. Lett.* **2011**, *13*, 4112−4115. (b) Ma, D.; Zavalij, P. Y.; Isaacs, L. Acyclic cucurbit[n]uril congeners are high affinity hosts. *J. Org. Chem.* **2010**, *75*, 4786−4795. (c) Ma, D.; Hettiarachchi, G.; Nguyen, D.; Zhang, B.; Wittenberg, J. B.; Zavalij, P. Y.; Briken, V.; Isaacs, L. Acyclic cucurbit[n]uril molecular containers enhance the solubility and bioactivity of poorly soluble pharmaceuticals. *Nat. Chem.* **2012**, *4*, 503−510. (d) Ma, D.; Zhang, B.; Hoffmann, U.; Sundrup, M. G.; Eikermann, M.; Isaacs, L. Acyclic cucurbit[n]uril-type molecular containers bind neuromuscular blocking agents in vitro and reverse neuromuscular block in vivo. *Angew. Chem., Int. Ed.* **2012**, *51*, 11358−11362. (e) Minami, T.; Esipenko, N. A.; Zhang, B.; Isaacs, L.; Nishiyabu, R.; Kubo, Y.; Anzenbacher, P. Supramolecular sensor for cancer-associated nitrosamines. *J. Am. Chem. Soc.* **2012**, *134*, 20021−20024. (f) Shen, C.; Ma, D.; Meany, B.; Isaacs, L.; Wang, Y. Acyclic cucurbit[n]uril molecular containers selectively solubilize single-walled carbon nanotubes in water. *J. Am. Chem. Soc.* **2012**, *134*, 7254−7257. (g) Minami, T.; Esipenko, N.; Akdeniz, A.; Zhang, B.; Isaacs, L.; Anzenbacher, P. Multi-analyte sensing of addictive over the counter (OTC) drugs. *J. Am. Chem. Soc.* **2013**, *135*, 15238−15243.

(12) Zhang, B.; Zavalij, P. Y.; Isaacs, L. Acyclic CB[n]-type molecular containers: Effect of solubilizing group on their function as solubilizing excipients. *Org. Biomol. Chem.* **2014**, *12*, 2413−2422.

(13) Tririya, G.; Zanger, M. Synthesis of anthracyclinone precursor: 5,12-dihydroxy-1,3,4-trihydronaphthacene-2,6,11-quinone. *Synth. Commun.* **2004**, *34*, 3047−3059.

(14) Murahashi, S.-I.; Miyaguchi, N.; Noda, S.; Naota, T.; Fujii, A.; Inubushi, Y.; Komiya, N. Ruthenium-catalyzed oxidative dearomatization of phenols to 4-(tert-butylperoxy)cyclohexadienones: Synthesis of 2-substituted quinones from p-substituted phenols. *Eur. J. Org. Chem.* **2011**, 5355−5365.

(15) Connors, K. A. *Binding Constants*; John Wiley & Sons: New York, 1987; pp 261−281.

(16) (a) Mock, W. L.; Shih, N.-Y. Structure and selectivity in host-guest complexes of cucurbituril. *J. Org. Chem.* **1986**, *51*, 4440−4446. (b) Adrian, J. C.; Wilcox, C. S. Chemistry of synthetic receptors and functional group arrays. 15. The effects of added water on thermodynamic aspects of hydrogen bond based molecular recognition in chloroform. *J. Am. Chem. Soc.* **1991**, *113*, 678−680.

(17) Higuchi, T.; Connors, K. A. Phase-solubility techniques. *Adv. Anal. Chem. Instrum.* **1965**, *4*, 117−212.

(18) (a) Fabre, C.; Mimura, N.; Bobb, K.; Kong, S.-Y.; Gorgun, G.; Cirstea, D.; Hu, Y.; Minami, J.; Ohguchi, H.; Zhang, J.; Meshulam, J.; Carrasco, R. D.; Tai, Y.-T.; Richardson, P. G.; Hideshima, T.; Anderson, K. C. Dual inhibition of canonical and noncanonical nf-*κ*b pathways demonstrates significant antitumor activities in multiple myeloma. *Clin. Cancer Res.* **2012**, *18*, 4669−4681. (b) Zhang, J.; Sliskovic, D. R.; Ducker, C. E. (Profectus Biosciences, Inc., USA). Preparation of oxabicyclo[4,1,0]heptenyl benzamide derivatives as nuclear factor-kb inhibitors and useful for treatment of various diseases. WO 2010148042, 2010. (c) Zhang, J.; Sliskovic, D. R.; Ducker, C. E. (Profectus Biosciences, Inc., USA). Preparation of benzamide and naphthamide derivatives for inhibition of nuclear factor-kb. WO 2010127058, 2010.

(19) (a) Huang, W.-H.; Zavalij, P. Y.; Isaacs, L. Cucurbit[n]uril formation proceeds by step-growth cyclo-oligomerization. *J. Am. Chem. Soc.* **2008**, *130*, 8446−8454.

(20) (a) Rekharsky, M. V.; Inoue, Y. Complexation thermodynamics of cyclodextrins. *Chem. Rev.* **1998**, *98*, 1875−1917. (b) Houk, K. N.; Leach, A. G.; Kim, S. P.; Zhang, X. Binding affinities of host-guest, protein-ligand, and protein-transition-state complexes. *Angew. Chem., Int. Ed.* **2003**, *42*, 4872−4897.